CILAMCE 2017
Florianópolis - Santa Catarina - Brazil

WORKING FLUID SELECTION AND OPTIMIZATION OF ORC FOR WHR IN CEMENT PRODUCTION PROCESS

Luiz Fernando Moreira

Felipe Raúl Ponce Arrieta

Elviro Pereira Barbosa Júnior

Gustavo Rodrigues da Costa Horta

luizfmoreira@hotmail.com

felipe.ponce@pucminas.br

juniorelviro@gmail.com

gustavohorta@live.com

Pontifical Catholic University of Minas Gerais

500, Dom José Gaspar Avenue, Belo Horizonte, 30.535-901, Minas Gerais, Brazil

Abstract. *The cement industry accounts for one of the highest electric energy consumption among all industrial sectors. The waste heat recovery (WHR) system provided by the organic Rankine cycle (ORC) is able to produce electricity from waste heat sources of the cement production process with no additional fuel consumption. This paper proposes a methodology for working fluid selection in order to select the most suitable organic fluids to perform on a real ORC. This approach is based on a fluids' safety and environmental characteristics, thermodynamic properties presented in an ideal ORC and their saturated vapour curves. Afterwards, real ORCs under subcritical and subcritical with superheating operating conditions were designed and optimized using the genetic algorithm method in Equation Engineering Solver (EES) software with the previous working fluids chosen. According to the proposed methodology, eight out of fifty-four organic fluids were designated as the most appropriate ones to work with the real ORC. In addition, results showed that the subcritical with superheating ORC performed better than the subcritical ORC in terms of net power output, thermal and exergy efficiencies. Moreover, the isentropic working fluid R141b achieved the greatest results in the subcritical ORC, while another isentropic fluid, R11, presented the highest effectiveness in the subcritical with superheating operating condition.*

Keywords: *Organic Rankine cycle, Waste heat recovery, Genetic algorithm, Cement industry*

1 INTRODUCTION

The cement industry has one of the greatest electric energy consumption levels among all industrial sectors. As reported by IFC (2014), the expenses with electricity correspond to approximately 25% of all operational costs in a cement plant. Additionally, it is possible to provide up to 30% of the total electric energy needs of a cement industry or supply low-grade heat for the production process using waste heat recovery (WHR) technologies, such as cogeneration systems. Aiming to decrease the energy consumption in the cement sector by generating electric energy with no additional fuel consumption and reducing CO_2 emissions, the energy cogeneration system provided by the organic Rankine cycle (ORC) has been emphasized as an attractive option. ORC is capable of producing electricity from waste heat sources derived from the preheater exhaust and clinker cooler exhaust gases with low-medium temperature (80 to 400ºC), which would be released into the atmosphere.

The main difference between ORC and the steam Rankine cycle (SRC) is that while the SRC works with water as its working fluid, the ORC operates with organic working fluids with low boiling points such as refrigerants, ethers, alcohols, etc. Due to the organic fluids' properties, ORC offers more advantages than SRC when working with temperatures between 80 and 400ºC, for example: good adaptability to different heat sources, simpler construction than other cycles for WHR, good efficiency, low operational and maintenance costs, good commercial availability (Eyidogan et al, 2016; Lecompte et al, 2015; Li, G., 2016; Tchanche et al, 2014; Wang, X. et al, 2015). The organic working fluid plays a key role in the ORC's operation, for it is directly related to the cycle performance. The main criteria adopted by the majority of researchers for selecting the most appropriate working fluids for ORC applications are the net power output and system efficiency. Furthermore, organic fluids can be classified according to their chemical composition, environmental and safety characteristics, and their saturation vapor curves.

Firstly, the organic working fluids can be categorized in accordance with their chemical composition in pure or zeotropic fluids. Pure fluids have a fixed chemical composition throughout, while zeotropic fluids are composed by a mixture of pure substances. As stated by Guo et al (2015), pure organic fluids are widely adopted due to their good chemical stability and easy availability of thermophysical properties. However, Dong et al (2014) explains that the main constraint on operating with pure organic fluids is its isothermal characteristic during the evaporation and condensation processes, which may not match the temperature profile of the heat source. Pu et al (2016) compared the net power output generated by an ORC operating with pure and zeotropic fluids. Results showed that the pure fluid was able to produce about 51.89% more net power output than the zeotropic fluid. On the other hand, Prasad et al (2015) optimized the composition of zeotropic working fluids, simulated an ORC with these zeotropic mixtures and compared the results with pure organic fluids. Results revealed that zeotropic fluids were thermally superior to pure fluids.

Secondly, the working fluids can be identified by their environmental and safety aspects. The environmental aspects are related to the impact on the environment of a substance, which are ODP (Ozone Depletion Potential) and GWP (Global Warming Potential) indexes. Whereas the safety aspects involve the cycle operational safety ruled by the ANSI/ASHRAE – 34/2007 standard and they are classified according to the substance toxicity and flammability (ASHRAE, 2009). Javanshir et al (2017) highlighted the importance of carefully analyzing these characteristics when choosing the organic working fluids for the ORC. In their study, Bao et al (2013) investigated and described important thermodynamic and physical properties in which working fluid selection should be based on.

Finally, the organic working fluids can be evaluated in accordance with their saturation vapor curves in (i) dry, with positive slopes; (ii) wet, with negative slopes; and (iii) isentropic, with nearly vertical saturation vapor curve (Li, C. et al, 2016). Long et al (2014) analyzed the influence of dry and isentropic organic fluids in the ORC exergy performance. Under subcritical operating condition, the authors found out that the highest exergy efficiency results were reached by fluids with lower critical temperatures. Li, X. et al (2014) compared the net power output generated by a simple ORC working with dry and wet organic fluids. It was stated by the authors that there is a range of temperatures below the critical point where it is possible to reach the maximum net power output. Nevertheless, there is also a reversion point where the net power output tends to decline for temperatures close to the critical one.

Also, the ORC can be categorized in consonance with its operating condition, which can be represented in the temperature–entropy (T-s) diagram, as (i) subcritical, in which the working fluid crosses the biphasic region at constant pressure lower than the pressure at the critical point; (ii) subcritical with superheating, which is similar to the subcritical condition, although the organic fluid is superheated before the turbine inlet; and (iii) supercritical, where the working fluid reaches a pressure and temperature higher than those ones at the critical point, that is, it passes from the liquid state to superheated vapor. A real ORC experiment was carried out by Gao et al (2014) using nine different organic fluids under subcritical and subcritical with superheating operating conditions. It was verified by the authors that, for all organic fluids analyzed, the subcritical with superheating condition showed best results in terms of thermal efficiency in comparison with the subcritical condition. Javanshir et al (2017) studied the correlation between the ORC operating condition and its efficiency according to the first law of thermodynamics. The authors explain that for the subcritical condition, the thermal efficiency is a quadratic function of the heat ratio of working fluid, in contrast with the subcritical with superheating and supercritical conditions, where this function is linear.

This study presents a methodology for working fluid selection with the purpose of selecting the most suitable organic fluids to perform on a real ORC. This procedure is based on a fluids' safety and environmental characteristics, thermodynamic properties obtained in an ideal ORC and their saturated vapor curves. Afterwards, real ORCs under subcritical and subcritical with superheating operating conditions were conceived and optimized using the genetic algorithm method in Equation Engineering Solver (EES) software with the working fluids chosen.

2 METHODOLOGY

The methodology for working fluid selection, as well as the ORC system specifications and its thermodynamic modeling are described as follows.

2.1 Working fluid selection

In order to determine the most adequate working fluids to be used in this work, five criteria for the elimination of the unsuitable organic fluids were established. These criteria are illustrated in Fig 1.

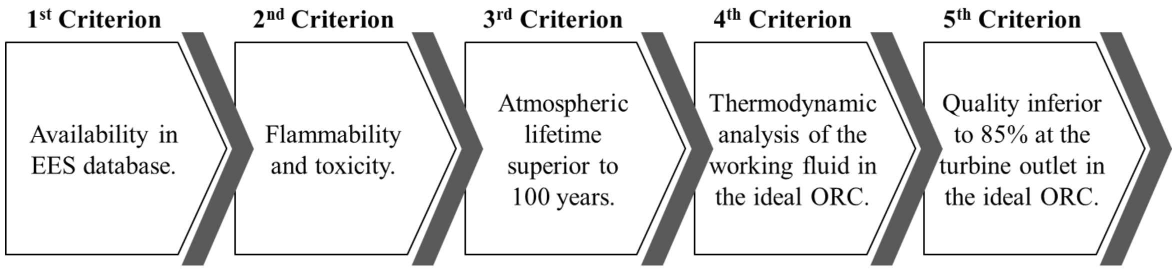

Figure 1. Established criteria for working fluids elimination

In accordance with the literature investigated, refrigerants are usually the most environmentally friendly among all working fluids eligible for operating in ORC. Based on this premise, 42 pure refrigerant fluids acquired from ASHRAE (2009), see Appendix 1, were considered and the availability of each one was evaluated in EES database, for it was the software used to perform the simulations. According to this criterion, 17 organic fluids, which their thermodynamic properties were not available in the software database, were eliminated. Table 1 shows the filtered fluids in this step, as well as their respective environmental and safety characteristics.

Table 1. Safety and environmental aspects of organic working fluids available in EES database

Fluid	Safety group	ODP	GWP_{100}	Atmospheric lifetime [years]
R11	A1	1	4,750	45
R12	A1	1	10,900	100
R13	A1	1	14,400	640
R22	A1	0.055	1,810	12
R23	A1	0	14,800	270
R32	A2	0	675	4.9
R113	A1	0.8	6,130	85
R114	A1	1	10,000	300
R116	A1	0	12,200	10,000
R123	B1	0.02	77	1.3
R124	A1	0.022	609	5.8
R125	A1	0	3,500	29
R134a	A1	0	1,430	14
R141b	-	0.11	725	9.3
R142b	A2	0.065	2,310	17.9
R143a	A2	0	4,470	52
R152a	A2	0	124	1.4
R218	A1	0	8,830	2,600
R227ea	A1	0	3,220	34.2
R236fa	A1	0	9,810	240
R245fa	B1	0	1,030	7.6
RC318	A1	0	10,300	3,200
R290	A3	0	~20	0.41
R600	A3	0	~20	0.018
R600a	A3	0	~20	0.019

In the second step, the working fluids were assessed based on their safety aspects. It was desired to work with fluids with null or low toxicity and flammability indexes, which means, fluids that belong to the safety groups A1, A2 and B1. However, as reported by Embraco (1996), the organic fluids R290, R600 and R600a, which belong to the group of non-toxic but highly flammable fluids (A3), are apt to be used because they do not offer risk of explosion due to their high dispersal speed into the air, not allowing a significant concentration of these gases in the environment for combustion to occur. Therefore, none of the fluids was disqualified at this stage.

In the third step, the working fluids were analyzed according to their environmental characteristics. Since all of them have very low or even zero ODP levels and varied indexes of GWP, atmospheric lifetime was used as a criterion for elimination. Thus, fluids with presence in the atmosphere longer than 100 years were removed, that is, R13, R23, R114, R116, R218, R236fa and RC318.

In the fourth step, the selected organic fluids were examined based on their properties and thermodynamic states presented after the simulation of an ideal ORC. Table 2 demonstrates the thermodynamic properties observed for the working fluid selection in this phase such as critical temperature (T_{cr}) and critical pressure (P_{cr}). Aiming to evaluate the thermodynamic characteristics of the fluids, a variation of 5°C was considered between the cooling water temperature at the condenser inlet and outlet. Then, a difference of 5°C between the outlet temperature of the cooling water and the working fluid temperature at the condenser outlet was adopted. Hence, the working fluid entered the condenser at environment temperature and left it at a temperature of 32°C. After this procedure, it was found that the saturation pressure at 32°C (P_{sat}) at the condenser outlet demonstrated by the fluid R113 was lower than the atmospheric pressure of 0.101 MPa. Consequently, this fluid was excluded from the next analysis, for this study does not propose to work with sub atmospheric pressures in the system.

Table 2. Thermodynamic properties of selected working fluids

Fluid	T_{cr} [°C]	P_{cr} [MPa]	P_{sat} at 32°C [MPa]
R11	198.00	4.41	0.130
R12	112.02	4.11	0.780
R22	96.13	4.99	1.260
R32	78.11	5.78	2.030
R113	214.06	3.39	0.060
R123	183.68	3.67	0.120
R124	122.28	3.62	0.470
R125	66.02	3.62	1.650
R134a	101.03	4.06	0.820
R141b	204.20	4.25	0.101
R142b	137.11	4.06	0.420
R143a	72.70	3.76	1.510
R152a	113.26	4.52	0.730
R227ea	102.80	3.00	0.560
R245fa	154.01	3.65	0.190
R290	96.68	4.25	1.130
R600	151.98	3.80	0.300
R600a	134.67	3.64	0.430

In the fifth and last step, each organic fluid selected up to this stage was evaluated according to its quality at the turbine outlet with the purpose of classifying their saturation vapor curves. Considering that the ideal ORC simulated worked with isentropic expansion in the turbine, twenty points of temperature were calculated at the turbine inlet along the saturated vapor line in the T-s diagram of each working fluid between the temperature at the condenser outlet and the temperature at the critical point. After analyzing the minimum and maximum quality values presented by the organic fluids at the turbine outlet, it was possible to identify the working fluids in consonance with the shape of their saturation vapor curves in wet, dry and isentropic fluids as exhibited in Fig. 2a, Fig. 2b and Fig. 2c, subsequently as examples. In addition, Table 3 shows the minimum and maximum quality at the turbine outlet of the organic fluids and their respective classification.

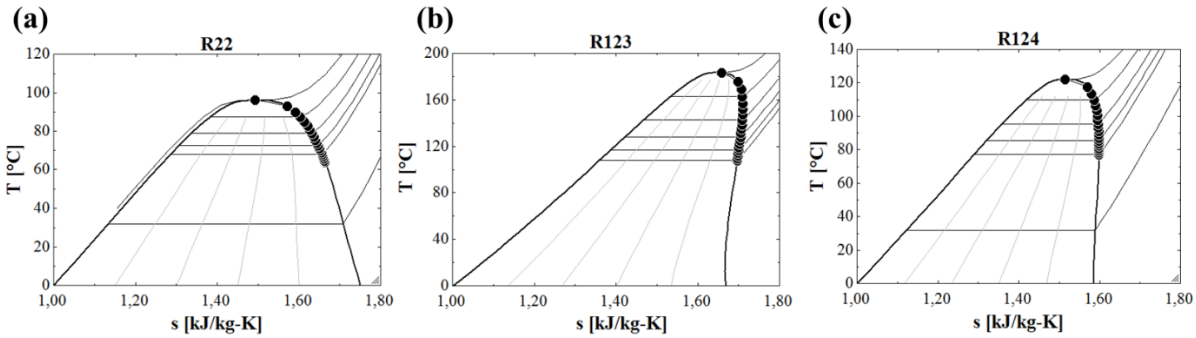

Figure 2. Saturation vapor curves of (a) wet, (b) dry and (c) isentropic organic working fluids

Table 3. Classification of organic fluids according to their quality at the turbine outlet

Fluid	Quality at the turbine outlet min - max[-]	Classification
R11	0.852 - 0.989	Isentropic
R12	0.745 - 0.970	Wet
R22	0.627 - 0.922	Wet
R32	0.535 - 0.885	Wet
R123	0.984 – 1.000	Dry
R124	0.959 - 1.000	Isentropic
R125	0.680 - 0.962	Wet
R134a	0.732 - 0.972	Wet
R141b	0.962 - 1.000	Isentropic
R142b	0.929 – 0.999	Isentropic
R143a	0.648 - 0.947	Wet
R152a	0.689 - 0.946	Wet
R227ea	0.986 - 1.000	Dry
R245fa	0.977 - 1.000	Dry
R290	0.731 - 0.972	Wet
R600	0.951 - 1.000	Isentropic
R600a	0.926 - 1.000	Isentropic

In order to avoid erosion on the turbine blades, the working fluids with quality under 85% at the turbine outlet were discarded. In other words, the wet fluids R12, R22, R32, R125, R134a, R143a, R152a and R290 were eliminated in this step. Moreover, the dry fluid R227ea was also removed due to be considered a "cold" fluid, it means that its critical temperature is near 100°C, so that the cycle operation with this fluid requires high pressure and temperature at the turbine inlet, making it unfeasible for this application. Finally, the most suitable organic fluids for this work are given in Table 4.

Table 4. Organic working fluids selected for application in this study

Fluid	Quality at the turbine outlet min - max[-]	Classification
R11	0.852 – 0.989	Isentropic
R124	0.959 – 1.000	
R141b	0.962 – 1.000	
R142b	0.929 – 0.999	
R600	0.951 – 1.000	
R600a	0.926 – 1.000	
R123	0.984 – 1.000	Dry
R245fa	0.977 – 1.000	

After selecting the most adequate working fluids for utilization in this study, the operating parameters of the ideal ORC were investigated. Aiming to adjust the results of the optimization performed afterwards with the working fluid selection in this section, during the temperature variation at the turbine inlet, it was identified in which pressure at that point it was possible to produce the greatest net power output amount for each working fluid. Therefore, this pressure, named optimum operating pressure ($P_{1,otm}$), was used as inlet data in the modeling of the real ORC proposed in this work.

2.2 System description and thermodynamic modeling

Energy from the suspension preheater exhaust gas and the hot air from the clinker cooler discharge were used simultaneously to generate electric energy. The analyzed configuration, a simple ORC, was comprised of a turbine (TURB), a condenser (COND), a pump (BB 01) and an evaporation unit composed of an economizer (ECO), evaporator 01 (EVP 01), evaporator 02 (EVP 02) and a superheater (SAQ). Additional components are the electric generator (GER), electrical substation (SEE) and electric motor (M). Figure 3 illustrates the ORC for WHR in a cement plant designed in this study.

The working principle of the proposed ORC can be explained as: the organic fluid receives heat in the evaporation unit at constant pressure (process 4-1); it experiences an isentropic expansion in the turbine (process 1-2); the working fluid rejects heat at constant pressure in the condenser (process 2-3); finally it is compressed isentropically in the pump (process 3-4) and returns to the evaporation unit to start a new cycle.

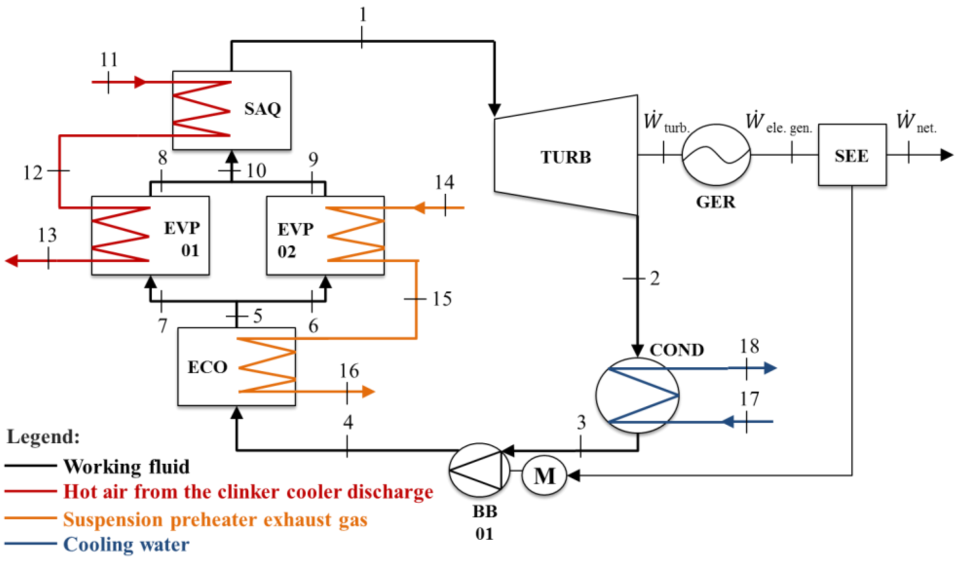

Figure 3. ORC for WHR in a cement plant

In accordance with the first and second laws of thermodynamic, the main operational parameters of the analyzed ORC were calculated as follow:

The heat received by the organic fluid in the evaporation unit can be expressed as Eq. (1):

$$\dot{Q}_{in\ cycle} = \dot{m}(h_1 - h_4) \tag{1}$$

where h_1 and h_4 are the specific enthalpies of the working fluid at the evaporation unit outlet and inlet, in this order; and $\dot{m}$ is the mass flow rate of organic fluid.

The power generated by the turbine is given by Eq. (2):

$$\dot{W}_{TURB} = \dot{m}(h_1 - h_2) \tag{2}$$

where h_1 and h_2 are the specific enthalpies of the working fluid at the turbine inlet and outlet, respectively.

The power consumed by the pump can be expressed as Eq. (3):

$$\dot{W}_{BB,01} = \dot{m}(h_4 - h_3) \tag{3}$$

where h_4 and h_3 are the specific enthalpies of the working fluid at the pump outlet and inlet, subsequently.

The net power output produced by the ORC is given by Eq. (4):

$$\dot{W}_{net} = \eta_{GEN}\dot{W}_{TURB} - \dot{W}_{BB,01} \tag{4}$$

where η_{GEN} is the efficiency of the electric generator.

The thermal efficiency of the ORC can be expressed as Eq. (5):

$$\eta_{th} = \frac{\dot{W}_{net}}{\dot{Q}_{in\ cycle}} \tag{5}$$

The physical exergy of each thermodynamic state is given by Eq. (6):

$$ex = h - h_0 - T_0(s - s_0) \quad (6)$$

where h is the specific enthalpy of the stream; h_0 is the specific enthalpy of the stream evaluated in the pressure and temperature of the dead state; T_0 is the temperature of the dead state (see Table 6); s is the specific entropy of the stream; and s_0 is the specific entropy of the stream evaluated in the pressure and temperature of the dead state.

The exergy destruction within the control volume by action of irreversibilities can be expressed as Eq. (7):

$$\dot{E}_d = T_0 \dot{\sigma}_{cv} \quad (7)$$

where $\dot{\sigma}_{cv}$ is the entropy generation inside the control volume.

The exergy efficiency of the ORC is given by Eq. (8):

$$\eta_{ex} = \frac{\dot{P}}{\dot{F}} \quad (8)$$

where $\dot{P}$ is the exergy product; and $\dot{F}$ is the exergy fuel.

The real cycle worked under subcritical and subcritical with superheating operating conditions. The chemical composition of the exhaust gases from cement production process as well as their outlet temperature from the evaporation unit were provided by Cimento Apodi (2015) as demonstrated in Table 5. This is a real cement plant located in Quixeré, CE, Brazil with a productive capacity of 3,500 tons of clinker per day.

Table 5. Exhaust gases from cement production process inlet data

Variable		Unit	Value
Hot air from the clinker cooler discharge data:			
Molar composition:	N_2	%	79.00
	O_2	%	21.00
Inlet temperature		ºC	440
Outlet temperature		ºC	114
Mass flow rate		kg/s	48.15
Suspension preheater exhaust gas data:			
Molar composition:	CO_2	%	26.30
	N_2	%	64.58
	O_2	%	4.94
	H_2O	%	4.18
Inlet temperature		ºC	310
Outlet temperature		ºC	228
Mass flow rate		kg/s	88.03

The isentropic efficiencies of the pump and turbine were acquired from Wang, J. et al (2009) and the main assumptions for the calculations of cogeneration systems commonly adopted in the investigated literature to perform the simulations are summarized in Table 6.

Table 6. Further inlet data considered in the modeling

Variable	Unit	Value
Isentropic efficiency of the pump	%	70.00
Isentropic efficiency of the turbine	%	85.00
Efficiency of the electric generator	%	98.50
Efficiency of the electric motor	%	99.00
Pressure of the exhaust gases from cement production process	MPa	0.101
Environment pressure (P_0)	MPa	0.101
Environment temperature (T_0)	ºC	22.00

Additionally, during the modeling of the ORC it was considered that: (i) the cycle was at steady state; (ii) all processes were adiabatic; and (iii) the variations of kinetic and potential energies were neglected. Furthermore, the simulations were performed using the software EES Professional V.10.092.

2.3 Optimization

As stated by Rao (2009), the optimization provided by the genetic algorithm is suitable for solving complex problems which involve multiple variables and non-linear or discrete functions. This method works based on principles of genetic and natural selection from the evolutionary theory proposed by Charles Darwin (1809-1882).

The optimization of the operating parameters of the cycle under subcritical and subcritical with superheating conditions aimed to find the highest results of net power output for each working fluid selected previously, for that reason, net power output was defined as the objective function. Table 7 exhibits the range of variation assumed during the optimization of the ORC operating parameters. Considering that the temperature difference at the economizer ($\Delta T_{sub\text{-}cooling}$) and evaporator 02 ($\Delta T_{EVP\ 02}$) were optimized in both operating conditions and the temperature variation at the turbine inlet ($T_{TURB\ in}$) and evaporator 01 ($\Delta T_{EVP\ 01}$) were optimized only in subcritical with superheating condition, the genetic algorithm method from EES library was set with 32 individuals, 64 generations and a mutation rate of 0.2625.

Table 7. Range of variation of the variables during the optimization

Fluid	$\Delta T_{sub\text{-}cooling}$ min – máx [°C]	$\Delta T_{EVP\ 01}$ min – máx [°C]	$\Delta T_{EVP\ 02}$ min – máx [°C]	$\Delta T_{TURB\ in}$ min – máx [°C]
R11	71 - 139	100 - 200	100 - 200	T_1 at $P_{1,otm}$ – 400°C
R123	111 - 130			
R124	74 - 78			
R141b	97 - 139			
R142b	84 - 91			
R245fa	96 - 103			
R600	91 - 100			
R600a	50 - 62			

3 RESULTS AND DISCUSSION

3.1 Ideal ORC

After simulating the ideal ORC for selecting the most appropriate organic fluids for this work, the main results obtained, as the optimum operating pressure and temperature at the turbine inlet, heat supplied to the cycle, specific net power output and first law efficiency, are given in Table 8.

Table 8. Results of the ideal ORC

Fluid	Classification	$P_{1,otm}$ [MPa]	T_1 [°C]	Q_{in} [kJ/kg]	W_{net} [kJ/kg]	η_{th} [%]
R11	Isentropic	3.674	185.36	222.16	53.19	23.94
R124		3.181	115.27	164.24	25.42	15.48
R141b		2.996	181.82	300.54	76.42	25.43
R142b		3.494	128.58	226.65	39.83	17.57
R600		2.974	137.23	467.29	108.17	23.15
R600a		2.859	120.44	405.80	79.72	19.65
R123	Dry	2.799	166.90	233.23	63.00	27.01
R245fa		2.813	139.96	245.52	56.46	23.00

From the point of view of power generation, results revealed that the working fluids with the greatest difference between the critical temperature and the temperature at the turbine inlet were the ones that produced the highest amounts of specific net power output, which are the isentropic fluids R600, R600a, R141b and the dry fluid R123. Also, it was discovered that for all the analyzed organic fluids, there was a temperature range in which the specific net power output generated by the cycle rises with the increase of the temperature at the turbine inlet. Nonetheless, the trend was inverted when this temperature approached the critical temperature of the working fluid. This result is illustrated in Fig. 4a.

From the energy perspective, the ideal ORC was more efficient when operating with higher temperatures at the turbine inlet. The organic fluids with critical temperature closer to the temperature of the heat source reached best results, that is, the dry fluid R123 and the isentropic fluids R141b and R11. Furthermore, the trend of the results was similar to that observed in the specific net power output produced by the cycle, which means, the thermal efficiency increased with the increment in the temperature at the turbine inlet. On the other hand, the first law efficiency was reduced when this temperature approached the critical temperature of the working fluid as shown in Fig. 4b. In contrast to the results of specific net power output generated by the cycle, the fluids R600 and R600a were not the most thermally efficient because they required higher heat input from the heat source due to their low critical temperatures compared to the other organic fluids.

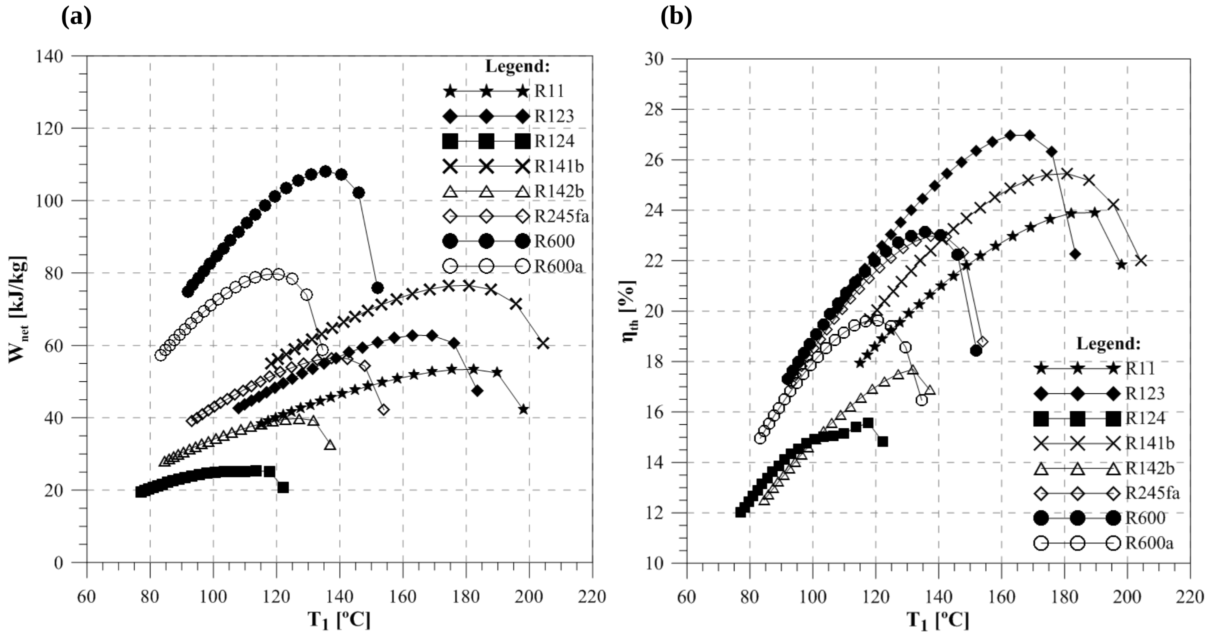

Figure 4. Results of the specific net power output (a) and thermal efficiency (b) for the ideal ORC with the temperature variation at the turbine inlet

3.2 Subcritical ORC

Applying the first and second laws of thermodynamics, continuity equation and inlet data, the real ORC was designed and optimized under the subcritical operating condition. The main results obtained as the heat supplied to the cycle, mass flow rate and specific volume (v) at the turbine inlet, net power output, exergy destruction thermal and exergy efficiencies are exposed in Table 9.

Table 9. Results for the real ORC under subcritical operating condition

Fluid	Classification	$\dot{Q}_{in}$ [kW]	$\dot{m}$ [kg/s]	v [m³/kg]	$\dot{W}_{net}$ [kW]	η_{th} [%]	η_{ex} [%]	$\dot{E}_d$ [kW]
R11	Isentropic	24,260	111.39	0.0038	4,537	18.70	41.52	6,391
R124		24,261	151.70	0.0034	2,876	11.85	26.31	8,053
R141b		24,261	82.11	0.0061	4,564	18.81	41.76	6,365
R142b		24,261	109.56	0.0045	3,303	13.62	30.23	7,625
R600		24,260	52.99	0.0104	3,552	14.64	32.50	7,377
R600a		24,260	61.20	0.0104	3,107	12.81	28.43	7,822
R123	Dry	24,261	105.81	0.0046	4,316	17.79	39.49	6,613
R245fa		24,261	100.82	0.0049	3,605	14.86	32.99	7,324

According to the results, the working fluids which provided the largest quantity of net power output and achieved the highest thermal and exergy efficiencies were the isentropic fluids R141b, R11 and the dry fluid R123, in this order. This result is divergent from that one observed in the ideal ORC, for this one takes into account the mass flow rate for power generation.

3.3 Subcritical with superheating ORC

Analogous to the subcritical operating condition, a similar approach was applied to the subcritical with superheating condition for simulating and optimizing the variables of the ORC. Table 10 presents the main results for the ORC working under this condition, for instance the heat supplied to the cycle, mass flow rate and specific volume at the turbine inlet, net power output, exergy destruction, first and second laws efficiencies.

Table 10. Results for the real ORC under subcritical with superheating operating condition

Fluid	Classification	$\dot{Q}_{in}$ [kW]	$\dot{m}$ [kg/s]	v [m³/kg]	$\dot{W}_{net}$ [kW]	η_{th} [%]	η_{ex} [%]	$\dot{E}_d$ [kW]
R11	Isentropic	24,256	79.42	0.0073	5,042	20.79	46.14	5,885
R124		24,203	98.00	0.0069	3,085	12.75	28.28	7,824
R141b		24,219	54.79	0.0117	4,768	19.69	43.68	6,147
R142b		24,165	68.49	0.0095	3,607	14.93	33.11	7,285
R600		24,197	39.48	0.0167	3,589	14.83	32.89	7,323
R600a		24,245	41.67	0.0180	3,135	12.93	28.70	7,788
R123	Dry	24,177	77.37	0.0078	4,376	18.10	40.12	6,531
R245fa		24,178	75.18	0.0080	3,656	15.12	33.54	7,243

Differently from the results reached in subcritical condition, the best organic fluids from the perspective of net power output, thermal and exergy efficiencies in this operating condition was the isentropic fluid R11 followed by the also isentropic fluid R141b and the dry fluid R123, respectively. It can be justified by the reduction in entropy generation in the components of the cycle provided by this superheated operating condition. In addition, the fluid R11 was the organic fluid that presented the most expressive decrease on exergy destruction (8.59%) compared to R141b (3.54%) and R123 (1.25%).

3.4 Subcritical X Subcritical with superheating ORC

Comparing the results of both operating conditions, it was verified that the subcritical with superheating ORC was more thermally and exergetically efficient than the subcritical ORC, in average, 4.50% and 4.43%, subsequently. Moreover, the subcritical with superheating operating condition produced, in average, 4.27% more net power output than the subcritical condition. As mentioned, the isentropic working fluid R141b achieved the greatest amount of thermal and exergy efficiencies and net power output in the subcritical ORC. Whereas, another isentropic organic fluid, R11, performed better in subcritical with superheating operating condition in terms of energy, exergy and net power output generated.

A comparison between the results of subcritical and subcritical with superheating operating conditions is illustrated in Fig. 5 from the point of view of net power output produced. The improvement in the results of the ORC operating under subcritical with superheating condition can be explained by the decline in mass flow rate and the increase in the temperature and specific volume at the turbine inlet for all working fluids evaluated. Furthermore, it was found that the reason why the fluid R11 generated more net power output compared to the other organic fluids was due to its higher temperature at the economizer inlet in the superheated condition.

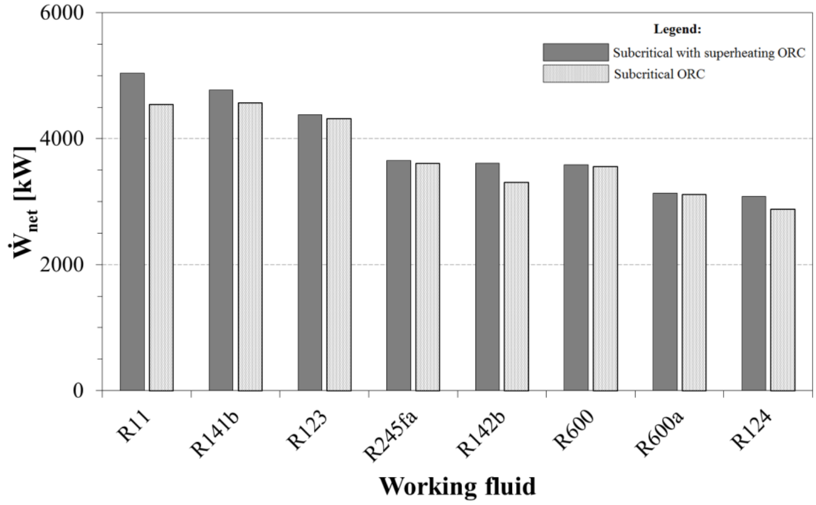

Figure 5. Comparison between subcritical and subcritical with superheating operating conditions results in terms of net power output

From the energy context, the increment in the temperature, specific volume and the decrease in mass flow rate at the turbine inlet in the subcritical with superheating condition led a decline in the heat input required by the ORC. Consequently, the thermal efficiency in this operating condition was slightly higher for all working fluids in comparison with the subcritical condition as demonstrated in Fig. 6.

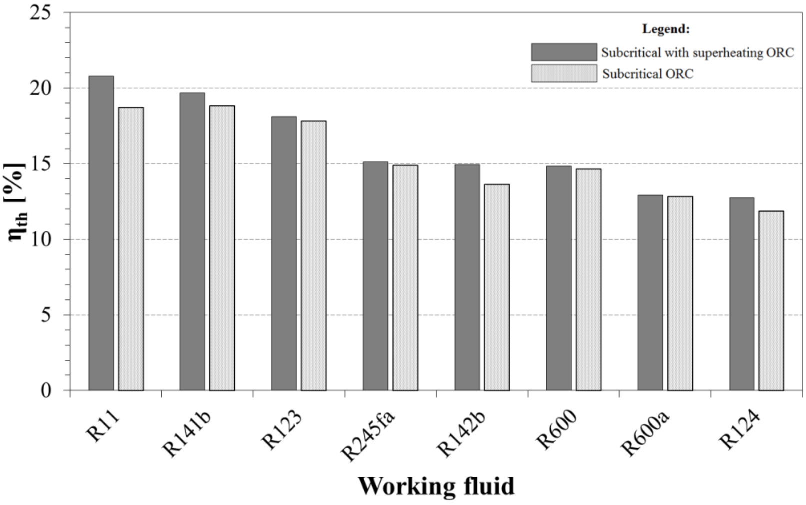

Figure 6. Comparison between subcritical and subcritical with superheating operating conditions results in terms of thermal efficiency

Lastly, Fig. 7 presents the exergy results for subcritical and subcritical with superheating operating conditions. In consonance with the net power output and thermal efficiency results, all organic fluids working under subcritical with superheating condition also performed exergetically better than operating under subcritical condition. This was due to the minimization of irreversibility losses provided by the decrease of the mass flow rate and the growth of the thermodynamic temperature and specific volume at the turbine inlet in this operating condition. Also, differently from the first law efficiency, which showed a modest improvement, most of the working fluids investigated experienced a larger increase in exergy efficiency, particularly the isentropic fluid R11.

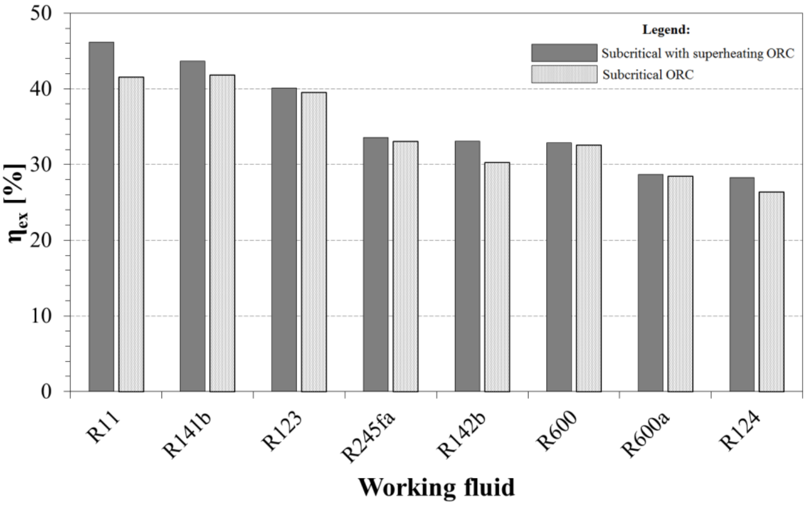

Figure 7. Comparison between subcritical and subcritical with superheating operating conditions results in terms of exergy efficiency

These results agree on what was stated by Moran et al (2013) that the effectiveness of the cycle with superheating is superior to the cycle without superheating due to its higher average temperature of heat addition. Hence, the operating condition, known as subcritical with superheating, permitted advantageous overall performance for the ORC.

4 CONCLUSIONS

The conclusions of the working fluid selection and optimization of ORC for WHR in cement production process are:

- The safety and environmental aspects of the working fluids are crucial factors to determine their viability to operate in the ORC;
- Operating parameters such as heat supplied to the cycle, temperature, pressure, mass flow rate and specific volume at the turbine inlet play a key role in the system performance;
- There is a temperature range at the turbine inlet and an optimum operating pressure where it is possible to obtain the maximum ORC overall effectiveness;
- The subcritical with superheating operating condition presented higher results compared to the subcritical condition from the point of view of net power output, thermal and exergy efficiencies;
- The isentropic fluid R141b performed better when working under subcritical operating condition, while the other isentropic fluid R11 achieved the highest results when the operating condition was subcritical with superheating.

Acknowledgements

The authors gratefully acknowledge the support provided by the Pontifical Catholic University of Minas Gerais (PUC Minas), the Coordination for the Improvement of Higher Education Personnel (CAPES) and the Foundation for Research Support of Minas Gerais (FAPEMIG).

REFERENCES

American National Standards Institute (ANSI), & American Society of Heating, Refrigerating and Air-Conditioning Engineers (ASHRAE), 2007. *ANSI/ASHRAE 34–2007: Designation and Safety Classification of Refrigerants*. ASHRAE.

American Society of Heating, Refrigerating and Air-Conditioning Engineers (ASHRAE), 2009. *Handbook Fundamentals.* ASHRAE.

Bao, J., & Zhao, L., 2013. A review of working fluid and expander selections for organic Rankine cycle. *Renewable and Sustainable Energy Reviews*, v. 24, pp.325-342.

Cimento Apodi, 2015. *Waste heat recovery system*. 15 slides: color.

Dong, B., Xu, G., Cai, Y., & Li, H., 2014. Analysis of zeotropic mixtures used in high-temperature Organic Rankine cycle. *Energy Conversion and Management*, v. 84, pp.253-260.

Embraco, 2017. *Informativo técnico: Isobutano (R600a) como refrigerante em sistemas herméticos de refrigeração*. Joinvile, Available: < http://www.embraco.com/DesktopModules/DownloadsAdmin/Arquivos/95035.pdf>. Access in: 19 mar. 2017.

Eyidogan, M., Kilic, F., Kaya, D., Coban, V., & Cagman, S., 2016. Investigation of Organic Rankine Cycle (ORC) technologies in Turkey from the technical and economic point of view. *Renewable and Sustainable Energy Reviews*, v. 58, pp.885-895.

Gao, W., Li, H., Xu, G., & Quan, Y., 2014. Working fluid selection and preliminary design of a solar organic Rankine cycle system. *Environmental Progress & Sustainable Energy*, v. 34, pp.619-626.

Guo, C., Du, X., Yang, L., & Yang, Y., 2015. Organic Rankine cycle for power recovery of exhaust flue gas. *Applied Thermal Engineering*, v. 75, pp.135-144.

International Finance Copororation (IFC), 2014. *Waste Heat Recovery for the Cement Sector: Market and Supplier Analysis*. Available: < http://www.ifc.org >. Access in: 12 jan. 2017.

Javanshir, A., & Sarunac, N., 2017. Thermodynamic analysis of a simple Organic Rankine Cycle. *Energy*, v. 118, pp.85-96.

Lecompte, S., Huisseune, H., Broek, M., & Paepe, M., 2015. Methodical thermodynamic analysis and regression models of organic Rankine cycle architectures for waste heat recovery. *Energy*, v. 87, pp.60-76.

Li, C., & Wang, H., 2016. Power cycles for waste heat recovery from medium to high temperature flue gas sources – from a view of thermodynamic optimization. *Applied Energy*, v. 180, pp.707-721.

Li, G., 2016. Organic Rankine cycle performance evaluation and thermoeconomic assessment with various applications part II: Economic assessment aspect. *Renewable and Sustainable Energy Reviews*, v. 64, pp.490-505.

Li, X., Zhao, W., Lin, D., & Zhu, Q., 2014. Working fluid selection based on critical temperature and water temperature in organic Rankine cycle. *Science China Technological Sciences*, v. 58, n. 1, pp.138-146.

Long, R., Bao, Y, Huang , X., & Liu, W., 2014. Exergy analysis and working fluid selection of organic Rankine cycle for low grade waste heat recovery. *Energy*, v. 73, pp.475-483.

Moran, M., Shapiro, H., Boettner, D., & Bailey, M., 2013. *Princípios de Termodinâmica para Engenharia*. LTC.

Prasad, G., Kumar, C., Murthy, S., & Venkatarathnam, G., 2015. Performance of an organic Rankine cycle with multicomponent mixtures. *Energy*, v. 88, pp.690-696.

Pu, W., Yue, C., Han, D., He, W., Liu, X., Zhang, Q., & Chen, Y., 2016. Experimental study on Organic Rankine cycle for low grade thermal energy recovery. *Applied Thermal Engineering*, v. 94, pp.221-227.

Rao, S., 2009. *Engineering optimization: Theory and practice*. John Wiley & Sons.

Tchanche, B., Pétrissans, M., & Papadakis, G., 2014. Heat resources and organic Rankine cycle machines. *Renewable and Sustainable Energy Reviews*, v. 39, pp.1185-1199.

Wang, J., Dai, Y., & Gao, L., 2009. Exergy analyses and parametric optimizations for different cogeneration power plants in cement industry. *Applied Energy*, v. 86, pp.941-948.

Wang, X., Li, X., Li, Y., & Wu, C., 2015. Payback period estimation and parameter optimization of subcritical organic Rankine cycle system for waste heat recovery. *Energy*, v. 88, pp.734-745.

APPENDIX 1 – Pure refrigerants eligible to perform on the ORC

Class	Code	Chemical nomenclature	Chemical formula
Methane	R11	Trichlorofluoromethane	CCl_3F
	R12	Dichlorodifluoromethane	CCl_2F_2
	R12B1	Bromochlorodifluoromethane	$CBrClF_2$
	R13	Chlorotrifluoromethane	$CClF_3$
	R14	Tetrafluoromethane	CF_4
	R21	Dichlorofluoromethane	$CHCl_2F$
	R22	Chlorodifluoromethane	$CHClF_2$
	R23	Trifluoromethane	CHF_3
	R30	Dichloromethane	CH_2Cl_2
	R31	Chlorofluoromethane	CH_2ClF
	R32	Difluoromethane	CH_2F_2
	R40	Chloromethane	CH_3Cl
	R41	Fluoromethane	CH_3F
	R50	Methane	CH_4
Ethane	R113	1,1,2-trichloro-1,2,2-trifluoroethane	CCl_2FCClF_2
	R114	1,2-dichloro-1,1,2,2-tetrafluoroethane	$CClF_2CClF_2$
	R115	Chloropentafluoroethane	$CClF_2CF_3$
	R116	Hexafluoroethane	CF_3CF_3
	R123	2,2-dichloro-1,1,1-trifluoroethane	$CHCl_2CF_3$
	R124	2-chloro-1,1,1,2-tetrafluoroethane	$CHClFCF_3$
	R125	Pentafluoroethane	CHF_2CF_3
	R134a	1,1,1,2-tetrafluoroethane	CH_2FCF_3
	R141b	1,1-dichloro-1-fluoroethane	CH_3CCl_2F
	R142b	1-chloro-1,1-difluoroethane	CH_3CClF_2
	R143a	1,1,1-trifluoroethane	CH_3CF_3
	R152a	1,1-difluoroethane	CH_3CHF_2
	R170	Ethane	CH_3CH_3
Ethers	RE170	Dimethyl ether	CH_3OCH_3
Propane	R218	Octafluoropropane	$CF_3CF_2CF_3$
	R227ea	1,1,1,2,3,3,3-heptafluoropropane	C_3HF_7
	R236fa	1,1,1,3,3,3-hexafluoropropane	$CF_3CH_2CF_3$
	R245fa	1,1,1,3,3-pentafluoropropane	$CF_3CH_2CHF_2$
	R290	Propane	$CH_3CH_2CH_3$
Cyclic	RC318	Octafluorocyclobutane	$(CF_2)_4$
Hydrocarbons	R600	Butane	$CH_3CH_2CH_2CH_3$
	R600a	Isobutane	$CH(CH_3)_2CH_3$
	R601	Pentane	$CH_3(CH_2)_3CH_3$
	R601a	Isopentane	$(CH_3)_2CHCH_2CH_3$
Oxygen	R610	Ethyl ether	$CH_3CH_2OCH_2CH_3$
	R611	Methyl formate	$HCOOCH_3$
Nitrogen	R630	Methyl amine	CH_3NH_2
	R631	Ethyl amine	$CH_3CH_2(NH_2)$